DISTRIBUTION OF WINDBLOWN SEDIMENT IN SMALL CRATERS ON MARS: PRELIMINARY WIND TUNNEL SIMULATIONS. R. L. Kienenberger[1], R. Greeley[1*], and D.A. Williams[1], [1]School of Earth and Space Exploration, Arizona State University, Tempe, AZ 85287 (Rebekah.Kienenberger@asu.edu), [*]Deceased.

Introduction: Many eroded secondary impact craters [1] or "hollows" [2] (<200 m in diameter) near the MER-Spirit rover landing site contain asymmetric deposits of windblown (aeolian) sediments (Figure 1). The deposits are located in the northwest section of the crater floor, which may indicate a prevailing wind direction toward the northwest (depositing material on the downwind side), or to the southeast (depositing material on the upwind side), indicating an area of reverse flow within the crater. By studying the location and characteristics of these deposits with respect to the crater morphometry, it may be possible to infer the predominant local wind direction during the deposition or redistribution of sediments. We present the preliminary results of wind tunnel simulations for comparison to HiRISE images and topographic data from a digital elevation model [3] in Gusev Crater as well as the results of a terrestrial analog field investigation at Amboy Crater, California [4].

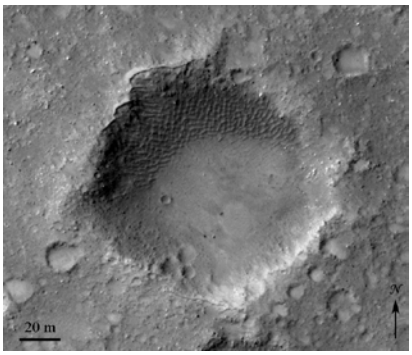

Figure 1. *MRO HiRISE image (PSP_001513_1655) showing a ~125m-in-diameter crater with aeolian deposits near the Spirit rover landing site.*

Methodology: Nine crater models were produced from acrylonitrile butadiene styrene (ABS), including a scaled model of an endogenic crater from the Amboy lava field, for experimentation using the Arizona State University Planetary Geology Wind Tunnel Facility, part of NASA's Planetary Aeolian Laboratory (PAL).

To scale the models to the boundary layer, grain size, and surface roughness, the models were produced with a vertical exaggeration of two [5]. The crater dimensions are presented in Table 1. To simulate the horizontal scale of the craters, runs were completed at low wind speeds (3.5 to 6 m/s) allowing multiple grain saltation paths within the crater. The rim heights and depths were chosen to represent the the average rim height-to-diameter ratios (r/D) and depth-to-diameter ratios (d/D) observed for the craters on Mars.

Crater	Depth* (m)	Diameter (m)	Rim Height* (m)	d/D Ratio*	r/D Ratio*
1	0.0160	0.152	0.0040	0.110	0.026
3	0.0065	0.152	0.0030	0.043	0.020
4	0.0100	0.253	0.0000	0.040	0.000
5	0.0050	0.152	0.0030	0.033	0.020
6	0.0030	0.152	0.0030	0.020	0.020
7	0.0065	0.152	0.0060	0.043	0.039
8	0.0065	0.152	0.0015	0.043	0.010
9	0.0065	0.152	0.0000	0.043	0.000

Table 1. *Morphometric properties of wind tunnel models using scaled vertical parameters (*).*

Model #1 was constructed to verify previous wind tunnel results of reverse flow and deposition on the upwind side of the crater floor for a deep crater with a pronounced rim [6]. Models #3, #5, and #6 were constructed with consistent diameters and rim heights but varying depths, which allowed an analysis of wind flow and sediment deposition as a function of the d/D. Models #7-9 were constructed with consistent diameters and depths but varying rim heights, which allowed a similar analysis of the r/D. Model #4 was constructed from a topographic profile of the largest endogenic crater at the Amboy field site for comparison to field results [4]. Profiles of the models are included in Figure 2.

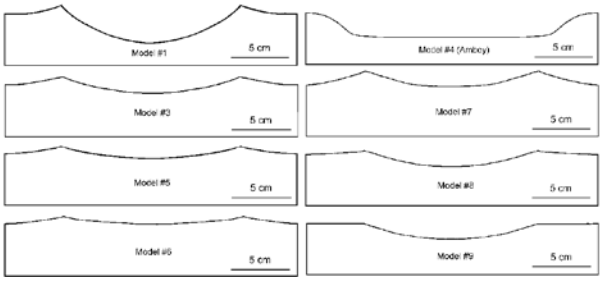

Figure 2. *Wind tunnel crater model profiles.*

A ridge of loose quartz sand was placed 1.2 m upwind of the test section. The crater models, crater holder (which allows for rotation of the models), and wind tunnel floor were coated with dyed-purple sand to provide a rough surface on the floor and contrast for the white sand. A grain size of 120 μm was used for the floor, model surfaces, and the upwind supply.

During each simulation, the free stream velocity was slowly increased from 2.5 m/s until sand could be seen saltating through the tunnel (generally 3.5 m/s). This velocity was maintained until the ridge reached equilibrium, at which time the velocity was slowly

increased. Velocities ranged from 3.5 to 9 m/s. The location and amount of deposition were observed and documented throughout the simulation. Images of the craters were taken from above the tunnel every two hours. These are referred to as the deposition runs.

Additional simulations were completed to determine how sediment moved in specific areas of the crater floor. A grid of small (8 mm in diameter by 3 mm high), conical sand piles was placed in and around the models (Figure 3). Each pile was monitored for particle movement relative to the wind direction. These simulations are referred to as the grid runs.

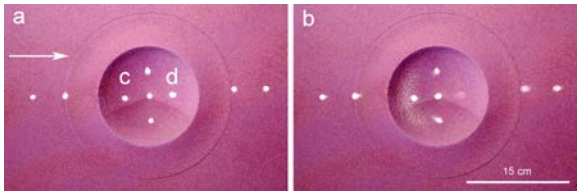

Figure 3. *Images (a) before and (b) after grid run with model #1. Piles outside the crater moved downwind and all piles within the crater moved upwind creating a deposit on the upwind side of the crater floor. Sand pile (c) represented an area of nearly stagnant wind while sand pile (d) represented an area of significant upwind movement. Wind direction and time sequence is from left to right.*

Preliminary Results: Based on the results of wind tunnel simulations, reverse flow occurred in eight of the nine crater models (#1-5, 7-9) with a d/D from 0.033 to 0.110 leading to sediment deposition on the upwind portions of the crater floors. Although model #6 (d/D=0.020, r/D=0.020) did not exhibit reverse flow, a deposit was noted on the upwind portion of the crater floor which likely corresponds to an area of stagnant wind observed during the grid run. Model #4 (d/D=0.40) represents a scaled model of an endogenic crater from the Amboy lava field. Although this model did not include a raised rim, reverse flow was observed in the upwind portion of the crater floor, leading to a deposit in this area during the deposition run (Figure 4). Thus, the depth of the crater likely plays a more important role than the rim height in the presence of reverse flow within craters. Previous field work at Amboy [4] resulted in an estimation that reverse flow ceases with a d/D from 0.02 to 0.05. Based on the wind tunnel simulations, reverse flow ceased at a d/D of ≤0.033. In addition, the area of the crater floor experiencing reverse flow decreased with shallower craters and lower rims, leading to smaller deposits on the upwind side.

Conclusions: Craters near the Spirit landing site with asymmetric aeolian deposits in the northwest portions of the craters have a range of d/D from 0.034 to 0.076, indicating reverse flow occurs in these craters. The location of windblown sediments in these craters suggests a prevailing wind from the northwest

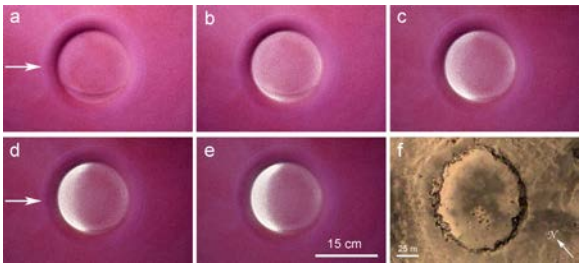

Figure 4. *Images a-e during deposition run with model #4 showing sediment on the upwind portion of the crater floor and (f) Google Earth image of the endogenic crater at Amboy lava field. Wind direction and time sequence is from left to right.*

to the southeast. Craters with low d/D ratios (<0.030) do not contain asymmetric deposits, indicating the sediments move directly over the crater floor in the downwind direction. However, the atmospheric pressure and gravity on Mars may play a role in the separation and reattachment of the wind flow. Therefore, these experiments should be conducted under Mars conditions to determine the effect of these parameters on the location and characteristics of the sediment deposits.

Future Work: A systematic analysis of the sharpness of the crater rim is being conducted to determine the effect of this parameter on wind flow over craters. Additionally, wind tunnel simulations will be conducted under Mars conditions to determine the influence of atmospheric pressure and gravity on the deposits. All results will be compared with HiRISE images and morphometric properties of craters on Mars to determine how wind patterns and the resulting aeolian deposition in and around small craters vary as a function of crater morphometry.

Acknowledgments: This research was funded by the NASA Planetary Geology and Geophysics Program and the JPL Mars Exploration Rover project.

References: [1] McEwen, A. S., et al. (2005), *Icarus* 176, 351-381. [2] Golombek, M. P., et al. (2006), J. of Geophys. Res., Vol. 111, E02S07, doi:10.1029/2005JE002503. [3] Kirk, R. L., et al. (2008), *J. of Geophys. Res.*, Vol. 113, E00A24, doi:10.1029/2007JE\003000. [4] Kienenberger, R. L. and R. Greeley (2012), Distribution of Windblown Sediment in Small Craters on Mars: Field Analog Studies at Amboy Crater, California. Planet. Space Sci., Vol. 68, Iss. 1, doi:10.1016/j.pss.2011.03.003. [5] Iversen, J. D., R. Greeley, B. R. White, and J. B. Pollack (1976), The Effect of Vertical Distortion in the Modeling of Sedimentation Phenomena: Martian Crater Wake Streaks, J. of Geophys. Res., Vol. 81(26), 4846 – 4586. [6] Greeley, R., J. D., Iversen, J. B. Pollack, N. Udovich, and B. White (1974), Wind tunnel studies of Martian aeolian processes, Proc. R. Soc. Lond. A., 341, 331 – 360.